Simulating the effect of boron doping in superconducting carbon

Yuki Sakai, James R. Chelikowsky, and Marvin L. Cohen

Phys. Rev. B **97**, 054501 — Published 1 February 2018

DOI: 10.1103/PhysRevB.97.054501

Simulating the effect of boron doping in superconducting carbon

Yuki Sakai,[1] James R. Chelikowsky,[1, 2, 3] and Marvin L. Cohen[4, 5]

[1] *Center for Computational Materials, Institute for Computational Engineering and Sciences, The University of Texas at Austin, Austin, Texas 78712, USA*

[2] *Department of Chemical Engineering, The University of Texas at Austin, Austin, Texas 78712, USA*

[3] *Department of Physics, The University of Texas at Austin, Austin, Texas 78712, USA*

[4] *Department of Physics, University of California at Berkeley, Berkeley, California 94720, USA*

[5] *Materials Sciences Division, Lawrence Berkeley National Laboratory, Berkeley, California 94720, USA*

(Dated: January 16, 2018)

Abstract

We examine the effect of boron doping in superconducting forms of amorphous carbon. By judiciously optimizing boron substitutional sites in simulated amorphous carbon we predict a superconducting transition temperature near 37 K at 14 % boron concentration. Our findings have direct implications for understanding the recently discovered high T_c superconductivity in Q-carbon.

I. INTRODUCTION

Doped carbon materials are known to be superconductors with relatively low values for T_c. For example, graphite intercalation compounds exhibit superconductivity[1] with alkali and alkaline-earth metal intercalant with a superconducting transition temperature T_c, up to 11.5 K in the case of CaC_6 under ambient pressure[2]. Alkali-doped fullerene (C_{60}) solids also exhibit superconductivity[3], *e.g.*, T_c is 33 K in the case of $Cs_xRb_yC_{60}$[4]. In addition to these sp^2-hybridized carbon materials, boron-doped sp^3-hybridized diamond is also known to be a superconductor[5]. The highest T_c experimentally for this material is 11.4 K[6] although the theoretically predicted potential T_c is approximately 55-80 K[7].

One obstacle in the realization of a high T_c is the limited amount of boron that can be doped in diamond. Recently, a T_c of 36.0 K has been reported when boron atoms are doped into a new amorphous form of carbon: *Q-carbon*[8,9]. The amount of boron doping reported is approximately 17 %. The T_c of this boron-doped Q-carbon is comparable to that of MgB_2 (39 K)[10]. However, the structural and electronic properties of boron-doped Q-carbon remain largely unknown in spite of its remarkable T_c.

Here we report the effect of boron doping into amorphous carbon in an attempt to understand Q-carbon and related materials. We replace the carbon atoms of a simulated amorphous carbon system with boron atoms one by one and find that the acceptor states can be either shallow or deep depending on surrounding geometries. We show that shallow acceptor states, which are important for achieving superconductivity in boron-doped diamond[11], can be realized when we properly choose specific substitutional sites. We also study the electron-phonon coupling in boron-doped amorphous carbon and show that those with shallow acceptor states can induce a superconductivity as in boron-doped diamond. We find a T_c of 37 K can be achieved at 14 at% boron with a resulting electron-phonon coupling constant, $\lambda = 1.11$. Even when we completely neglect the electron-phonon coupling of low-frequency vibrational modes, which is often an artifact of a computational simulation, the T_c is 26 K at 12.5 %doping case.

II. COMPUTATIONAL METHOD

We employ a total energy pseudopotential approach with Troullier-Martins norm-conserving pseudopotentials[12–14] constructed within density functional theory (DFT)[15,16] using the local density approximation (LDA)[17,18]. The real-space pseudopotential DFT code PARSEC is used for molecular dynamics (MD) simulations and structural determination of amorphous carbon[19–22]. Once the structure is determined, the plane-wave DFT package Quantum ESPRESSO[23] is used for phonon and electron-phonon coupling calculations based on density functional perturbation theory[24,25] with Γ-only sampling. The McMillan equation as modified by Allen and Dynes is adopted to estimate the T_c from λ, logarithmic average phonon frequency $\omega_{log} = \exp(\langle \ln\omega \rangle)$, and the Coulomb repulsion parameter $\mu^* = 0.12$[26]. See Supplemental Material for the detailed information on DFT calculations[27].

We perform first-principles Born-Oppenheimer MD simulations as implemented in the PARSEC code first to obtain randomized atomic coordinates of liquid-like carbon[27]. A cubic cell with 64 carbon atoms is employed to model the amorphous system. We pick up different randomized atomic coordinates, *i.e.*, snapshots at various time steps of the above MD run and "quench" those coordinates to obtain an amorphous structure. It has been argued that a higher density coupled with a faster quenching rate generally give a larger portion of 4-fold coordinated atoms in amorphous carbon[28–30]. Based on the dominant 4-fold coordination observed in Q-carbon[8], we choose a relatively high density of 3.4 g/cm^3 (lattice constant of the cubic cell is 7.21 Å) that is close but lower than that of diamond to obtain 4-fold-rich amorphous carbon structure. In addition, we immediately quench (relax) the structure from a randomized carbon atoms to achieve high 4-fold coordination.

III. RESULTS AND DISCUSSION

A. Properties of amorphous carbon

The amorphous carbon studied here is the lowest energy structure among several different structures generated by the above procedure (see Supplemental Material for the atomic coordinates)[27]. The coexistence of the 3- and 4-fold coordinated atoms can be seen in the ball-and-stick model and can be also recognized by the broad peak around 1.5 Å in the radial

distribution function [see Figs. 1(a) and 1(b)]. This structure contains 81 % (12 atoms of 64 atoms) of 4-fold-coordinated carbon atoms and rest is 3-fold (we use 1.8 Å as the criterion for the coordination). This value is close to the experimental observed high sp^3 ratio of 85 % in Q-carbon[9].

We find the density of states of the amorphous carbon to have several localized states near the Fermi energy as shown in Fig. 1(c). These localized electronic states predominantly consist of p-orbitals of the 3-fold coordinated carbon atoms as the projected density of states (blue dashed line) indicates. The p_z-orbital of 3-fold carbon atoms in amorphous carbon cannot form a π-network as in graphite particularly when the 3-fold atom is surrounded by 4-fold atoms. The proximity of 3-fold and 4-fold atoms form localized states in the gap region. Even when a 3-fold carbon atom is not completely isolated, the atom can be seen as a defect in a 4-fold dominated carbon system. Such an imperfect sp^3-hybridization causes the shoulder-like feature around the gap edges as well.

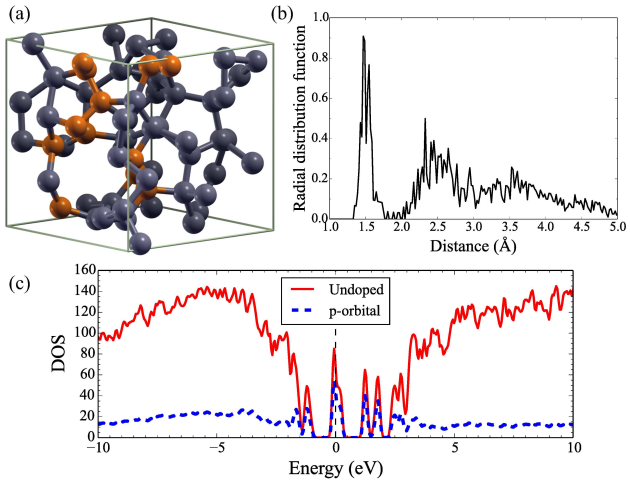

FIG. 1. (Color online) (a) Ball-and-stick model of amorphous carbon. Orange and gray spheres represent 3-fold and 4-fold coordinated carbon atoms, respectively. (b) Radial distribution function of amorphous carbon. (c) Density of states (in states/spin/Ry/cell) of undoped amorphous carbon (red solid line) and its projection onto p-orbital of 3-fold coordinated carbon atoms (blue dashed line). The vertical dashed line at 0 eV indicates the Fermi level. A Gaussian broadening width and energy grid of 0.05 eV is used.

B. Electronic properties of boron-doped amorphous carbon

We systematically replaced carbon atom sites with boron atoms to investigate the effect of substitutional boron doping on electronic and superconducting properties[31]. An important feature in superconducting boron-doped diamond is hole doping, owing to shallow acceptor states close to the occupied states[11]. However, in amorphous carbon, and presumably Q-carbon, the position of the acceptor states strongly depends on the geometries of substitutional sites. For example, the relative energy of the highest occupied state in our simulation for the undoped case (the 128th state) measured from a reference state (*e.g.*, the 123rd state when the target doping amount is 9 or 10) is 2.12 eV at the Γ point in the first Brillouin zone. This relative energy of the 128th state varies from 1.54 eV in one site to 2.54 eV in a different site when we substitute one of the 64 carbon atoms with a boron atom. (See the top panel of Fig. 2). Therefore, there is no trivial way to obtain a dominant hole-doped electronic structure. One needs to carefully choose substitutional sites.

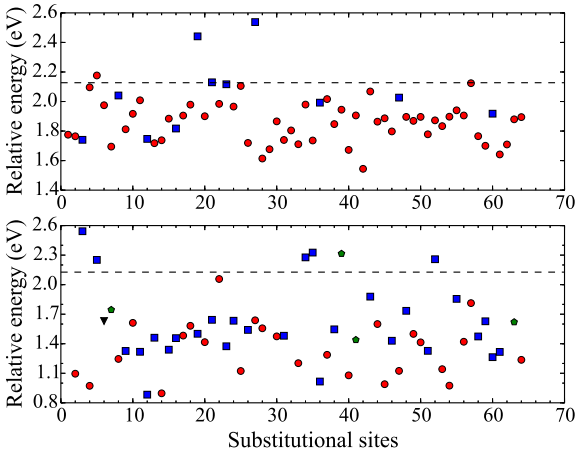

FIG. 2. (Color online) Site dependence of relative Kohn-Sham eigenvalue energies of C_{64} to BC_{63} case (top panel) and B_5-S1 to B_6 case (bottom panel). Black triangles, blue squares, red circles, and green pentagons represent 2-fold, 3-fold, 4-fold, and 5-fold coordination, respectively (2-fold is almost 4-fold since it has two nearest-neighbor atoms at a distance slightly longer distance than 1.8 Å. Here the energy difference between 128th and 123rd states are plotted. The horizontal dashed line shows the corresponding value in the undoped case. Here the eigenvalues are computed using an LDA exchange-correlation functional and could be altered when one uses a different functional (see Supplemental Material)[27].

Based on this observation: (1) Substitutional sites are chosen so that the 128th state becomes low compared with the reference state (123rd state here) at the Γ point when the lowering is significant. (2) If the lowering is not significant, we use the Γ-point energy eigenvalues to screen possible substitutional sites. (3) We compute the density of states to further screen the sites in question. (4) The electron-phonon coupling constant of the optimized candidate structure is computed. This reduces the number of electron-phonon coupling calculations, which can be computationally intensive.

We investigate a favorable substitutional site to create shallow acceptor states from Fig. 2. From C_{64} to BC_{63}, the "best" ten substitutional sites are all 4-fold coordinated as expected. Eight of these best 10 sites have 4-fold coordinated nearest-neighbor atoms. In addition, the nearest-neighbor distance is less than 1.64 Å and in 6 cases, the distance is less than 1.60 Å. On the other hand, the half of the "worst" ten sites are 3-fold coordinated. The rest is 4-fold-coordinated, but four of the five remainder has a long nearest neighbor distance above 1.7 Å. The other one has two 3-fold coordinated atoms in its nearest neighbor. This result indicates 3-fold coordinated sites are generally unfavorable to create shallow acceptors.

The distribution of eigenvalues is also analyzed in one of the cases from B_5C_{59} to B_6C_{58} to assess the interaction with preexisting boron atoms (the bottom panel of Fig. 2). Seven of the worst ten sites are 3-fold coordinated, and two 4-fold coordinated sites turn a preexisting 4-fold B atom into 3-fold atom. On the other hand, eight of the best ten sites are 4-fold coordinated and preexisting boron atoms remain 4-fold in most cases although a few are 5-fold coordinated. The other two sites have a boron atom at 1.8 Å and 2.0 Å, and can be virtually regarded as 4-fold coordinated considering the size of boron atom. In addition, a 3-fold coordinated boron-dimer creates a deep acceptor state in the 5th site while a 4-fold boron dimer in the 47th site creates a shallow state. Therefore, the creation of 3-fold coordination is again not favored and 4-fold coordination is favored even when boron dimers are formed.[32].

Figure 3 illustrates the evolution of the densities of states of boron-doped amorphous carbon starting from B_4-S1 to B_9-S1 structures following the procedure explained above. Here Sx represent a series of doped structures. In principle, the Fermi level becomes deep compared with the band edge as we increase the number of boron atoms. The exception is the case from B_7S1 to B_8S1 where the state at the relative energy of the band-edge state around 1 eV becomes shallower. In the B_9-S1 case, the 128th state become deeper (above

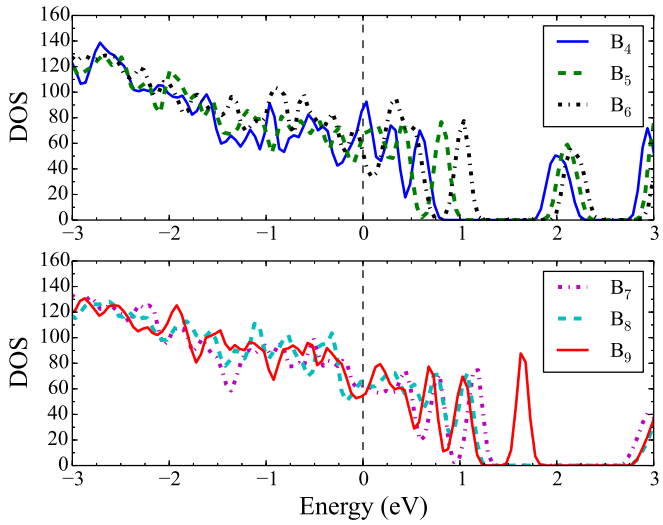

FIG. 3. (Color online) Densities of states (DOS, in states/spin/Ry/cell) of B_4-S1 (blue solid), B_5-S1 (green dashed), B_6-S1 (black dash-dotted), B_7-S1 (magenta dash-dotted), B_8-S1 (cyan dashed), and B_9-S1 (red solid) structures.

1.5 eV) because the 59th site is 3-fold coordinated and it creates a relatively localized state as will be discussed below. Consequently, we are able to obtain shallow acceptor states in boron-doped amorphous carbon by properly selected substitutional doping.

C. Superconducting properties of boron-doped amorphous carbon

Table I lists the structure, λ, square and logarithmic average frequency ω_{log} and $\omega_2 = \sqrt{\langle\omega^2\rangle}$, T_c, and Fermi level density of states N_{E_F} of various boron-doped amorphous carbon. In principle, λ and T_c increases as the number of dopants increases while the ω_{log} decreases. Starting from the B_4-S1 case (T_c of 15 K), the T_c becomes 19, 23, 26, and 33 K. The highest T_c of 37 K is achieved in the 14 % doping case, which is comparable to the experimentally measured T_c of boron-doped Q-carbon.[9] Table I also lists another series of boron-doped amorphous carbon starting from B_4-S2 structure to show that another doped structure exhibits electron-phonon coupling as well.

Despite their high density of states, low doping structures such as B_4C_{60} and B_5C_{59} cases do not exhibit strong electron-phonon interaction. As we described in Fig. 1(c), the original electronic states around Fermi level comes from p-orbital of 3-fold coordinated carbon atoms. This orbital character remains similar even when, for example, four boron atoms are doped.

TABLE I. Electron-phonon coupling constant (λ), logarithmic average frequency (ω_{log}), square average frequency (ω_2), superconducting transition temperature T_c, and density of states at the Fermi energy (N_{E_F}, in states/spin/Ry/cell) of various boron-doped amorphous carbon systems. A branch in series Sx is represented with an alphabet suffix as Sx_a. The values in the parentheses are those without the contribution from low-frequency vibrational modes. The convergence check of these parameters with respect to the Gaussian broadening width and atomic coordinates of the structures are provided in Supplemental Material[27].

Structure	λ	ω_{log} (K)	ω_2 (K)	T_c (K)	N_{E_F}
		B_4 (6.2 %)			
S1	0.64 (0.41)	593 (839)	850 (1034)	13 (2)	69.0
S2	0.47 (0.44)	807 (840)	1029 (1053)	5 (4)	71.3
		B_5 (7.8 %)			
S1	0.67 (0.49)	603 (770)	865 (997)	16 (6)	61.1
S2	0.56 (0.50)	769 (852)	1003 (1058)	11 (7)	57.8
		B_6 (9.4 %)			
S1	0.69 (0.58)	672 (807)	920 (1000)	19 (13)	50.8
S2	0.63 (0.52)	677 (830)	955 (1042)	15 (9)	61.3
		B_7 (10.9 %)			
S1	0.76 (0.60)	635 (753)	880 (971)	23 (14)	63.1
S2	0.87 (0.50)	454 (835)	801 (1048)	22 (8)	69.4
		B_8 (12.5 %)			
$S1_a$	0.89 (0.62)	509 (801)	798 (1002)	26 (16)	60.0
$S1_b \equiv S3$	0.96 (0.76)	606 (731)	841 (933)	35 (26)	80.7
S2	1.20 (0.62)	372 (764)	718 (988)	31 (15)	71.3
		B_9 (14.1 %)			
$S1_a$	0.92 (0.64)	577 (778)	825 (984)	31 (18)	58.6
$S3_a$	1.27 (0.68)	414 (735)	708 (942)	37 (20)	70.1
$S3_b$	1.11 (0.71)	494 (737)	777 (956)	37 (22)	60.3

The Γ point wavefunction of the 128th state exhibits an almost localized feature around 3-fold coordinated atoms. The 127th state also has non-negligible amplitude around 3-fold coordinated atoms. Even though the doping creates shallow acceptor levels, these states still do not contribute to the electron-phonon coupling. Therefore, it is important to increase the "effective" density of states that contributes to the electron-phonon coupling to obtain metalic covalency in boron-doped amorphous carbon, as in the other high T_c covalent superconudctors[33].

In fact, λ slightly increases from 0.89 to 0.92 although we put a boron atom in a 3-fold coordinated site of B_8-S1 structure to make the B_9-S1 structure. This doping creates a localized state around 1.5 eV as shown in the bottom panel of Fig. 3, but the effective acceptor states does not decrease since the Fermi energy is deep enough in the occupied states. The formation of the 3-fold coordinated boron atom also modifies the phonon density of states as can be seen in the increase of the ω_{log} from 509 to 577 K. Eventually the T_c also increases from 26 to 31 K. This result interestingly suggests some 3-fold coordination should be allowed in a relatively high-density boron doping case.

Figure 4 shows the Eliashberg spectral function $\alpha^2F(\omega)$ of B_4-S1 (blue line) and B_9-S1 (red line) structures. Comparing these two spectral functions, increasing boron doping raises the spectral weight for almost the entire frequency range. The spectral functions also show that spectral weight in low-frequency region is relatively large and irregular in the frequency region around 10 THz. The low-frequency oscillations occur because we compute λ at only the Γ point. Including contributions from other q-points should decrease the large contribution from particular modes. In fact, when we compute the electron-phonon interaction of B_8-S1 case on $2 \times 2 \times 2$ q-grid and $4 \times 4 \times 4$ k-grid, the $\alpha^2F(\omega)$ becomes more regular and broadened, and the spectral weight in higher-frequency modes become more substantial (see Fig. S4 in Supplemental Material)[27]. The λ, ω_{log}, and T_c calculated from this spectral function are 0.80, 586 K, and 24 K, respectively. This λ is slightly smaller than the Γ only calculation (0.89), but ω_{log} becomes larger (509 K in the Γ case), resulting in an almost similar value of T_c. Therefore, Γ-only sampling should be an acceptable approximation particularly in estimating T_c.

In Table I, superconducting parameters without the contribution from low-frequency optical phonon modes are also listed. Here the lowest-frequency mode and modes with frequencies less than 250 cm^{-1} are neglected. This is a rough approximation that reduces the

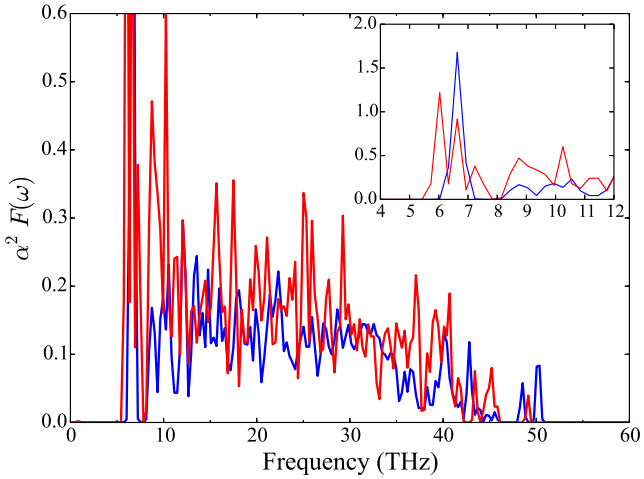

FIG. 4. (Color online) Eliashberg spectral function $\alpha^2F(\omega)$ of B_4-S1 (blue line) and B_9-S1$_a$ (red line) structures. The inset shows the magnified view of the low-frequency region.

spurious contribution from a particular low-frequency mode. From the $2\times2\times2$ q-grid results on B_8-S1 case discussed above, these values are considered to be the worst-case scenario and the values computed with a sufficient number of q-points should be in between those with and without the lowest-frequency optical mode. Nonetheless, the highest value of T_c in this approximation is 26 K in 12.5 % doped case and still comparable to the experimental T_c of boron-doped Q-carbon.

We note that an imaginary frequency acoustic branch appears when we compute the phonon dispersion relation with a $2 \times 2 \times 2$ q-grid in the cases of 12.5 % boron doped case (Fig. S3 in Supplemental Material)[27]. We attribute its origin to our artificially imposed cubic symmetry and to the restricted number of atoms. A similar geometry might appear under the extreme experimental condition such as high temperature melting and quick quenching in Q-carbon.

IV. SUMMARY

In summary, we have shown that a simulated model of boron-doped amorphous carbon, such as Q-carbon, is a superconductor when properly doped with shallow acceptor states. Our highest T_c of 37 K in 14 % boron doped case obtained here is comparable to that observed in boron-doped Q-carbon. Shallow acceptor states appear when doped boron atoms are 4-

fold coordinated even when boron dimers are formed. On the other hand, 3-fold boron atoms are generally not favored since they create deep acceptor states, but interestingly can increase T_c through an increase in ω_{log} in a relatively high doping case. The maximum T_c could be 26 K when we do not include the contribution from low-frequnecy modes, but it is still sizable. The procedure used here and findings should be useful for designing doped amorphous carbon with interesting physical properties. The present theoretical verification of high T_c in such a covalent light-element amorphous material produced under extreme high-temperature/rapid-quenching would imply that a material under an extreme condition could be a promising superconductor as seen in the recently-reported hydrogen sulfide under high pressure[34].

ACKNOWLEDGMENTS

YS and JRC acknowledge support from the U.S. Department of Energy (DoE) for work on nanostructures from grant DE-FG02-06ER46286, and on algorithms by a subaward from the Center for Computational Study of Excited-State Phenomena in Energy Materials at the Lawrence Berkeley National Laboratory, which is funded by the U.S. Department of Energy, Office of Science, Basic Energy Sciences, Materials Sciences and Engineering Division under Contract No. DE-AC02-05CH11231, as part of the Computational Materials Sciences Program. Computational resources are provided in part by the National Energy Research Scientific Computing Center (NERSC) and the Texas Advanced Computing Center (TACC). MLC acknowledges support from the National Science Foundation Grant No. DMR-1508412 and from the Theory of Materials Program at the Lawrence Berkeley National Lab funded by the Director, Office of Science and Office of Basic Energy Sciences, Materials Sciences and Engineering Division, U.S. Department of Energy under Contract No. DE-AC02-05CH11231. MLC acknowledges useful discussions with Professor Jay Narayan.

[1] N. B. Hannay, T. H. Geballe, B. T. Matthias, K. Andres, P. Schmidt, and D. MacNair, Phys. Rev. Lett. **14**, 225 (1965).

[2] T. E. Weller, M. Ellerby, S. S. Saxena, R. P. Smith, and N. T. Skipper, Nature Phys. **1**, 39 (2005).

[3] A. F. Hebard, M. J. Rosseinsky, R. C. Haddon, D. W. Murphy, S. H. Glarum, T. T. M. Palstra, A. P. Ramirez, and A. R. Kortan, Nature (London) **350**, 600 (1991).

[4] K. Tanigaki, T. W. Ebbesen, S. Saito, J. Mizuki, and J. S. Tsai, Nature (London) **352**, 222 (1991).

[5] E. A. Ekimov, V. A. Sidorov, E. D. Bauer, N. N. Mel'nik, N. J. Curro, J. D. Thompson, and S. M. Stishov, Nature (London) **428**, 542 (2004).

[6] Y. Takano, T. Takenouchi, S. Ishii, S. Ueda, T. Okutsu, I. Sakaguchi, H. Umezawa, H. Kawarada, and M. Tachiki, Diamond and related materials **16**, 911 (2007).

[7] J. E. Moussa and M. L. Cohen, Phys. Rev. B **77**, 064518 (2008).

[8] J. Narayan and A. Bhaumik, J. Appl. Phys. **118**, 215303 (2015).

[9] A. Bhaumik, R. Sachan, and J. Narayan, ACS Nano **11**, 5351 (2017).

[10] J. Nagamatsu, N. Nakagawa, T. Muranaka, Y. Zenitani, and J. Akimitsu, Nature (London) **410**, 63 (2001).

[11] K.-W. Lee and W. E. Pickett, Phys. Rev. B **73**, 075105 (2006).

[12] M. L. Cohen, Phys. Scr. **T1**, 5 (1982).

[13] J. Ihm, A. Zunger, and M. L. Cohen, J. Phys. C **12**, 4409 (1979).

[14] N. Troullier and J. L. Martins, Phys. Rev. B **43**, 1993 (1991).

[15] P. Hohenberg and W. Kohn, Phys. Rev. **136**, 864 (1964).

[16] W. Kohn and L. J. Sham, Phys. Rev. **140**, 1133 (1965).

[17] D. M. Ceperley and B. J. Alder, Phys. Rev. Lett. **45**, 566 (1980).

[18] J. P. Perdew and A. Zunger, Phys. Rev. B **23**, 5048 (1981).

[19] J. R. Chelikowsky, N. Troullier, and Y. Saad, Phys. Rev. Lett. **72**, 1240 (1994).

[20] J. R. Chelikowsky, J. Phys. D **33**, R33 (2000).

[21] L. Kronik, A. Makmal, M. L. Tiago, M. M. G. Alemany, M. Jain, X. Huang, Y. Saad, and J. R. Chelikowsky, Phys. Status Solidi B **243**, 1063 (2006).

[22] A. Natan, A. Benjamini, D. Naveh, L. Kronik, M. L. Tiago, S. P. Beckman, and J. R. Chelikowsky, Phys. Rev. B **78**, 075109 (2008).

[23] P. Giannozzi, S. Baroni, N. Bonini, M. Calandra, R. Car, C. Cavazzoni, D. Ceresoli, G. L. Chiarotti, M. Cococcioni, I. Dabo, A. Dal Corso, S. de Gironcoli, S. Fabris, G. Fratesi, R. Gebauer, U. Gerstmann, C. Gougoussis, A. Kokalj, M. Lazzeri, L. Martin-Samos, N. Marzari, F. Mauri, R. Mazzarello, S. Paolini, A. Pasquarello, L. Paulatto, C. Sbraccia, S. Scandolo,

G. Sclauzero, A. P. Seitsonen, A. Smogunov, P. Umari, and R. M. Wentzcovitch, J. Phys. Condens. Matter **21**, 5502 (2009).

[24] S. Baroni, S. de Gironcoli, A. dal Corso, and P. Giannozzi, Rev. Mod. Phys. **73**, 515 (2001).

[25] F. Giustino, Rev. Mod. Phys. **89**, 015003 (2017).

[26] P. B. Allen and R. C. Dynes, Phys. Rev. B **12**, 905 (1975).

[27] See Supplemental Material for the detailed information.

[28] N. A. Marks, D. R. McKenzie, B. A. Pailthorpe, M. Bernasconi, and M. Parrinello, Phys. Rev. B **54**, 9703 (1996).

[29] D. G. McCulloch, D. R. McKenzie, and C. M. Goringe, Phys. Rev. B **61**, 2349 (2000).

[30] J. Han, W. Gao, J. Zhu, S. Meng, and W. Zheng, Phys. Rev. B **75**, 155418 (2007).

[31] It is difficult to obtain even metallic boron-doped amorphous carbon when we randomize and quench atomic coordinates of B and C coexisting system. We usually obtain deep localized impurity states, resulting in semiconductors.

[32] Boron substitution also modifies the geometry of surrounding atoms because the amorphous structure has more room for relaxation than crystal. This significantly modifies the electronic properties as well, and it is still difficult to predict a favorable site to create shallow acceptor beforehand.

[33] N. Bernstein, C. S. Hellberg, M. D. Johannes, I. I. Mazin, and M. J. Mehl, Phys. Rev. B **91**, 060511(R) (2015).

[34] A. P. Drozdov, M. I. Eremets, A. I. Troyan, V. Ksenofontov, and S. I. Shylin, Nature **525**, 73 (2015).